


# Preliminary geochemical study of thermal waters at the Puracé volcano system (South Western Colombia): an approximation for geothermal exploration

Esteban Gómez-Díaz<sup>1\*</sup>; María Isabel Marin-Cerón<sup>1</sup>

DOI: <http://dx.doi.org/10.18273/revbol.v40n1-2018003> 

**Forma de citar:** Gómez-Díaz, E., y Marin-Cerón, M.I. (2018). Preliminary geochemical study of thermal waters at the Puracé volcano system (South Western Colombia): an approximation for geothermal exploration. *Boletín de Geología*, 40(1), 43-61. DOI: 10.18273/revbol.v40n1-2018003.

## ABSTRACT

The Puracé Volcano is located in the Cauca department, SW of Colombia, along the Coconucos volcanic chain. This volcano is an interesting target for geothermal exploration, because it is a young caldera-type volcano, with thermal activity (e.g. hot springs and fumaroles). Using hydro-geochemical analyses of hot springs, we determine the type of water, origin and relation with the geothermal system, reservoir temperature, mixing process and finally the potential areas for future exploration. The analyzed water-types are bicarbonate, dilute-chloride, sulphate-chloride, acid-sulphate and heated steam-acid sulfated. The conservative elements, allow to identify the correlation between different springs and to infer commune sources. Moreover, the applied solutes geothermometers for each suitable thermal-water group were used to estimate the reservoir temperature. The Silica geothermometers resulted within a range of 120°C -170°C while those the Cation geothermometers are above these temperatures reflecting values from 160°C to 220°C. However, the Cation geothermometer of low temperature clearly identify another zone of lower temperature. Mixing and recharge processes, were identified through of stable isotopes. Finally, the preliminary geothermal model shows two zones of high enthalpy system (>150°C).

**Keywords:** Puracé volcano; Hot Springs; Hydrogeochemistry; Geothermometers; High enthalpy system.

## Estudio geoquímico preliminar de aguas termales en el sistema volcánico Puracé (suroccidente colombiano): una aproximación para la exploración geotérmica

## RESUMEN

El Volcán Puracé está ubicado en el departamento de Cauca, al sur de Colombia en la cadena volcánica Coconucos. Este volcán es un interesante *target* para la exploración geotérmica, ya que es un volcán joven de tipo caldera, con actividad térmica (p.e. aguas termales y fumarolas). Usando análisis hidrogeoquímico de aguas termales, se determinó el tipo de agua, origen y relación con el sistema, temperatura del yacimiento, proceso de mezcla y finalmente las áreas potenciales para futuras exploraciones. Los tipos de agua analizados fueron: bicarbonatadas, cloruradas-diluidas, cloruradas - sulfatadas, ácido sulfatadas y aguas sulfatadas con vapor de agua caliente. Los elementos conservadores, permitieron identificar la correlación entre los diferentes manantiales e inferir fuentes comunes. Los geotermómetros de solutos aplicados para cada grupo de agua termal definido, permitieron estimar la temperatura del yacimiento. Los resultados de geotermómetros de Sílice, se encuentran dentro de un rango de 120°C -170°C mientras que los geotermómetros de Cationes están por encima de estas temperaturas reflejando valores de 160°C a 220°C. Sin embargo, el geotermómetro de Cationes de baja temperatura identifica claramente otra zona de menor temperatura. Los procesos de mezcla y recarga fueron dilucidados a través de isótopos estables. Finalmente, el modelo geotérmico preliminar muestra dos zonas de sistema de alta entalpía (>150°C).

**Palabras clave:** Volcán Puracé; Fuentes termales; Hidrogeoquímica; Geotermómetros; Sistema Alta Entalpía.

<sup>1</sup> Grupo Geología Ambiental e Ingeniería Sísmica, Universidad EAFIT, Medellín, Colombia.  
(\*): [egomezdl@eafit.edu.co](mailto:egomezdl@eafit.edu.co); [mmarince@eafit.edu.co](mailto:mmarince@eafit.edu.co)

## INTRODUCTION

Colombia is a country with high volcanic activity, due to the subduction of the Nazca plate below the North Andean Block (NAB), along the Pacific fire belt, developing a great potential for geothermal studies. Recent studies and developments in Colombia have been done by the Geological Colombian Service (GCS), synthetized at the National Inventory of Hot Springs (2012) <http://hidrotermales.sgc.gov.co/>. A preliminary study done by Garzón *et al.* (2004), indicate that the most water in Colombia are far from equilibrium, indicating that more detailed studies are much needed.

In spite of this, Colombia does not have electricity generation using geothermal energy yet. In recent years, several factors have been combined to identify sites with geothermal potential such as: (1) the energy crisis associated with global climate change and population growth; (2) global and regional initiatives that promote Geothermal development in Latin America and the Caribbean regions; (3) the recognition of geothermal areas as a competitive energy source for the region. As it is well known, the geothermal systems can be categorized in two different ways, either by temperature or enthalpy (high (>150 °C) vs low (<150 °C)) (Nicholson, 1993) or by geologic and tectonic association. The latter

can be split into four broad groups of geothermal systems (Chandrasekharam and Bundschuh, 2008): (1) Geothermal systems associated with active volcanism and tectonism; (2) continental collision; (3) active volcanism in continental rift systems; and (4) rift systems not associated with volcanism.

In this paper, we want to discuss about the Puracé Volcano System (PVS), located at the North Andean Volcanic Zone (NVZ), which is associated with active volcanism and tectonism (Nazca plate subduction-related system); the PVS, is generally high temperature/high enthalpy systems (>150°C), where the associated magma bodies provide the heat source.

The PVS is located in the Central Andean Cordillera of Colombia, along the Coconucos volcanic chain, which belongs to the so-called North Andean Volcanic Zone (NVZ) in the Andean mountain range. The PVS belongs to Puracé and Coconucos municipalities, at 35 km from Popayán city to the west. The geographic coordinates are 2 ° 19'01 N and 76 ° 23 '53 W (FIGURE 1). The Puracé volcano is an active volcano build over the old Pre-Puracé volcano, which in turn, developed inside of huge caldera called Paletará. The volcano presents fumarole activity which is located close to interior of the crater; there is also an important fumarole field, NW to the outer flank of the PVS.

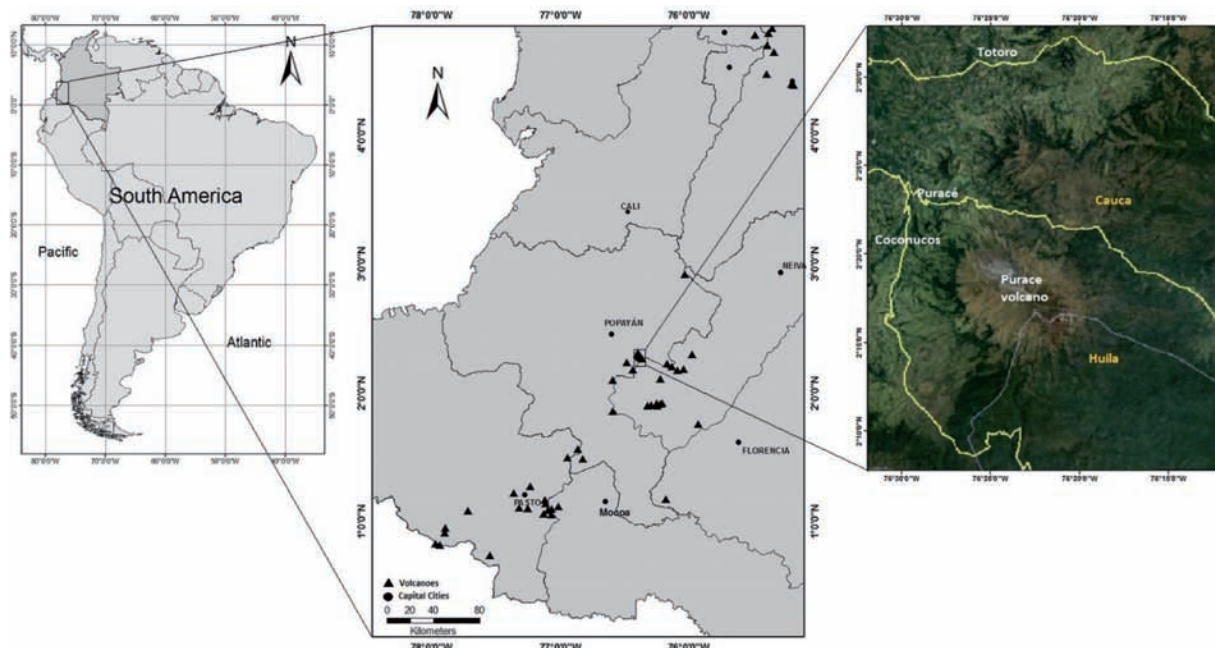


FIGURE 1. Puracé Volcano System (PVS) Location map.

## CONCEPTUAL FRAMEWORK

### Analyses tools

Waters forming geothermal fluids, may be derived from a variety of sources (e.g. Ellis and Mahon, 1977; Nicholson, 1993): (1) Meteoric water - surface water, that has travelled to depths of several kilometers through permeable horizons and fractures; (2) Connate or formation water ('Fossil' waters) - water buried with host sediments which has been out of contact with the atmosphere for long geological periods; (3) Juvenile water ('new') - water derived from primary rock magma, not previously part of the hydrosphere; (4) Metamorphic water - specially modified connate water derived from hydrous minerals during their recrystallization to less hydrous minerals during metamorphism; (5) Magmatic water - Water derived from magma that may not necessarily be juvenile water, because magma may incorporate deep circulating meteoric water or water from sediments.

The studies developed during the 1980s and early 1990s (e.g. Giggenbach, 1988), permitted the understanding of hydrothermal systems around the world, using the concentrations of dissolved ions, allowing to infer different diagrams, to determine the fluid-rock interaction process, to classify the different thermal waters types and in turn, to study the chemical-reactions involved in the formation and dissolution of the minerals that are in the systems. These diagrams are known as ion-plots (e.g. Tsch, Tc1b, Tc1f, Tnkm), and are presented as follow:

- 1) The Tcsh- ternary plot uses the  $\text{SO}_4\text{-Cl-HCO}_3$  anions (Giggenbach, 1988). This plot allows to understand the origin of the fluids and/or the processes that the geothermal fluid has undergone. Sulphate-waters are generally of volcanic origin associated with the condensation of geothermal gases. Chloride-waters are usually associated with balanced mature waters; they are very common in geothermal systems and present Cl concentrations ranging from hundreds to thousands of ppm. Finally, Bicarbonate-waters are related to water-mixtures with bicarbonate rich groundwater. In some cases, the mixture between meteoric and groundwaters, results in bicarbonated ones, with low concentration of Cl.
- 2) The Tc1b and Tc1f- ternary plots, define the relative content of the more conservative elements (e.g. Cl, B, Li, F), present in thermal waters. An

example is the lithium that is a conservative metal because it is less affected by secondary processes, so it use to be a good element to evaluate the origin (Giggenbach, 1991). The Tc1f plot is similar to Tc1b, but graphs Fluoride anions against Cl and B instead of Li cations. These plots are used to relate the springs and identify commune source of the water springs.

The Tnkm plot or triangular Plot of Giggenbach, uses the  $\text{Na}^+$ ,  $\text{K}^+$  and  $\text{Mg}^{+2}$  cations, it allows to establish the physical-chemical balance between the fluid and the host rock making it possible to estimate the temperature of the reservoir through of maturity of the waters associated with the hydrothermal system.

In general, several authors use these diagrams along with isotopic studies to classify waters in the geothermal system around the world to define characteristics of interest for geothermal exploration. These diagrams together with models are used to identify the reaction processes that govern the generation of balanced waters. Finally, knowing the temperature of the reservoir through the use of geothermometers is vital for studies in the geothermal exploration. The estimation of the temperatures helps to estimate the geothermal potential. The Solute geothermometer is a method based on empirical analytical equations in chemical reactions between the geothermal fluid and the minerals at depth and it is one of the most commonly used and it is divided in Silica geothermometers and Cation geothermometers. The Silica geothermometer is based on experimentally determined variations in the solubility of different silica species in water as a function of temperature within a range of 20 to 250°C (Chandrasekharam and Bundschuh, 2008). The limit of 250°C is due to silica dissolving and precipitating rapidly at higher temperatures, not allowing the concentration of silica in solution to remain constant as fluids are discharged at the surface (Nicholson, 1993). On the other hand, the Cation geothermometers are based on ion exchange and reactions using temperature dependent equilibrium constants (Chandrasekharam and Bundschuh, 2008). Due to the long residence time of geothermal fluids and constant high temperatures in geothermal reservoirs water-rock reactions attain equilibrium. At high temperatures these temperature dependent fluid equilibrium reactions are common; an example of this is the reaction involving Albite ( $\text{Na}$  feldspar) and geothermal fluids rich in  $\text{K}^+$  ions (O'Brien, 2010).

Through the geothermometers is possible to make Geoindicators (e.g. Xkmc & Xkms plots). These geoindicators organize the plotted data dots in a manner that illustrates both the evidence that supports the interpretation of equilibrated water at high temperature and the influence of shallow processes, and possible equilibrium at lower temperature (Powell and Cumming, 2010). Both geoindicators are proposed by Giggenbach and Goguel (1989), although these cross-plots are made with geothermometers, they can be interpreted more as geoindicators plots because they juxtapose and compare the potassium magnesium geothermometer with other values. In the case of Xkmc graph, it juxtaposes and compares the potassium-magnesium geothermometer with a measure of the partial pressure of CO<sub>2</sub> based on the equilibrium between K-feldspar, calcite and K-mica on one side and dissolved Ca<sup>+2</sup> and K<sup>+</sup> on the other (Giggenbach and Goguel, 1989). The Xkms graph is also a cross-plot of the K-Mg geothermometer, but uses the silica geothermometers (conductive) instead.

Therefore, the study of the chemical and isotopic composition of thermal manifestations may allow knowing the type of waters, the origin of fluids, the inferred temperatures at depth, the relationship between hydrothermal fluids and hydrology and hydrogeology and the interaction between fluid and rock. Moreover, studying the hot springs in a geothermal system requires to consider the percolation of meteoric waters from the recharge zones which, upon heating, react with the host rock, dissolving it and adding a large amount of chemical components to the geothermal fluid (e.g. Giggenbach, 1991).

### **Geological settings**

The PVS is associated to a metamorphic basement (Cajamarca Complex) in fault-contact with Cretacic volcanic rocks (Quebradagrande Complex), intruded by porphyritic Tertiary volcanic rocks (Maya and González, 1995). The main products of the volcanic activity are pyroclastic rocks, interspersed with lava flows of andesitic composition. The volcanic sequence at the west flank of the PVS consists essentially of the lava flow deposits, accompanied by the pyroclastic deposits. These deposits were associated to the Chagartón activity and caldera formation, possibly belonging to the Popayan Formation (Torres *et al.*, 1999), and/or the Chagartón Member of the Coconucos Formation (Monsalve, 2000).

The PVS, is controlled by N - S faults. These faults are associated with the Romeral and Cauca-Patía fault system, controlling the recent volcanic activity (Bohorquez *et al.*, 2005). The N-NW and N-NE fault trends, are clearly recognized and are represented by the Moras fault and the Coconucos fault. Using remote sense (p.e. satellite images and aerial photos) a morphological analysis was performed to detect lineaments and structures. The FIGURE 2 illustrate the geological map modified from Marquínez *et al.* (2003). The map shows lineaments with trend NW-SE between 6 and 11 km in length, which is controlled apparently by the San Jerónimo fault, and Mora fault. These lineaments are controlling some thermal emanations; therefore, the geothermal fluid flows may be controlled by permeable zones associated probably with distensive faults.

### **Hydrology**

The PVS area offers great water production related to the most important Colombian Andes rivers (e.g. Cauca and Magdalena rivers, located to the W and E, respectively). The hydrographic network, is very diversified due to the heterogeneity of its relief and configuration of the mountain system, the drainage varies from parallel to sub parallel type, which may be controlled by the faults systems (FIGURE 3). The middle river sizes, generally, run through deep canyons, due to the broken and steep shapes of the relief. The soils at the PVS region vary from moderately deep to deep and well drained according to the document: Management Plans Areas System of the National Parks of Colombia, the annual precipitation oscillates between 1500 and 2500 mm, based on the IDEAM hydro-meteorological data base.

The PVS area is influenced mainly by several watersheds such as the Vinagre river, Rio Grande, San Francisco, Anambio, Changue (Cauca river drainage system) and San Marcos and Bedon rivers (Magdalena river drainage system). Numerous hot springs are identified in the PVS area; they were divided into 4 groups (A, B, C, D), related to the above-mentioned watersheds systems (e.g. Grande, Vinagre, Bedon, Palace and Cobre). The group D contains the El Salado spring, that falls out of the watershed, however it was considered because its physical and chemical characteristic is very similar to the group D springs.

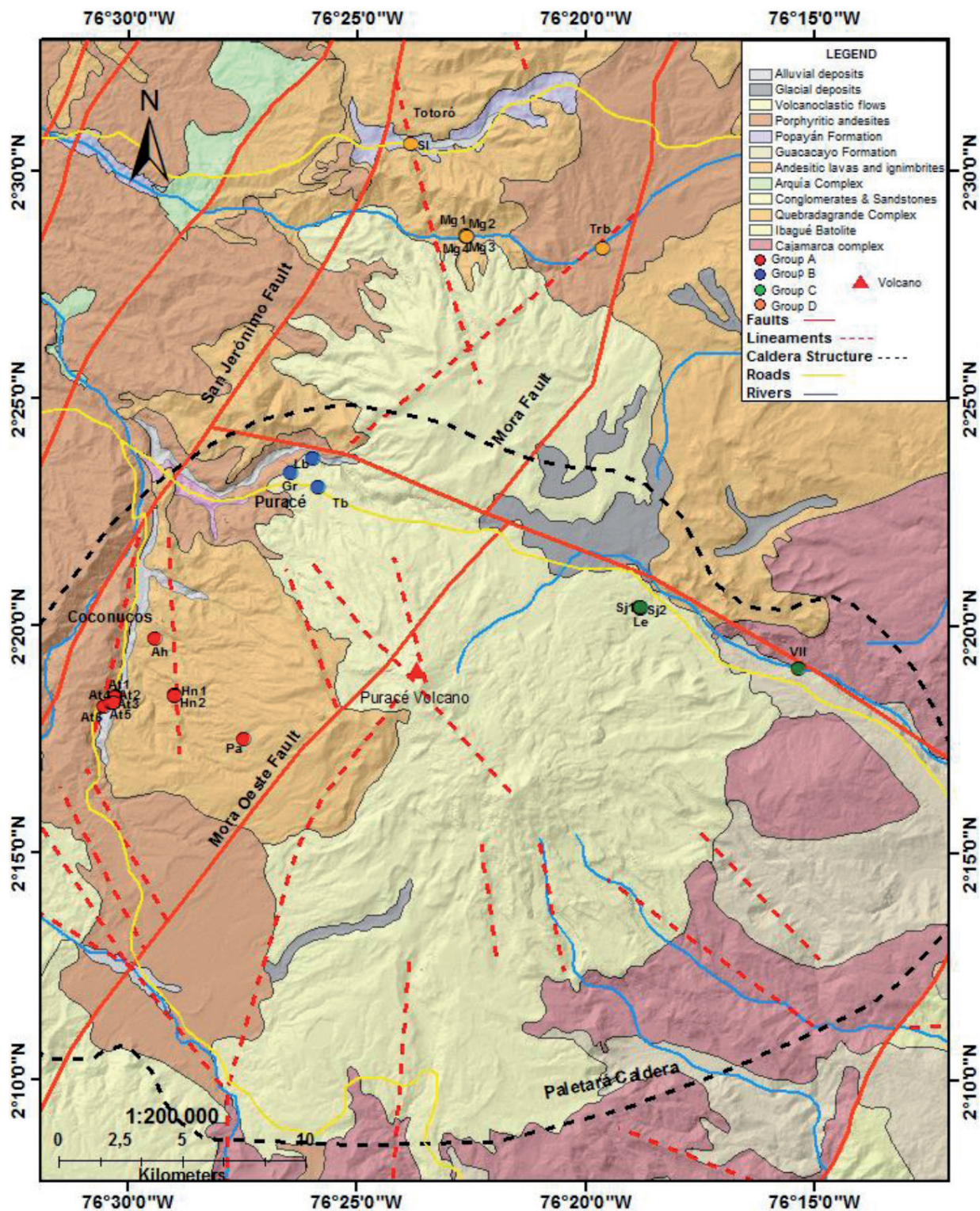


FIGURE 2. PVS geological and structure map with sample locations modified from Marquínez *et al.* (2003) geological map 365 Coconucos.

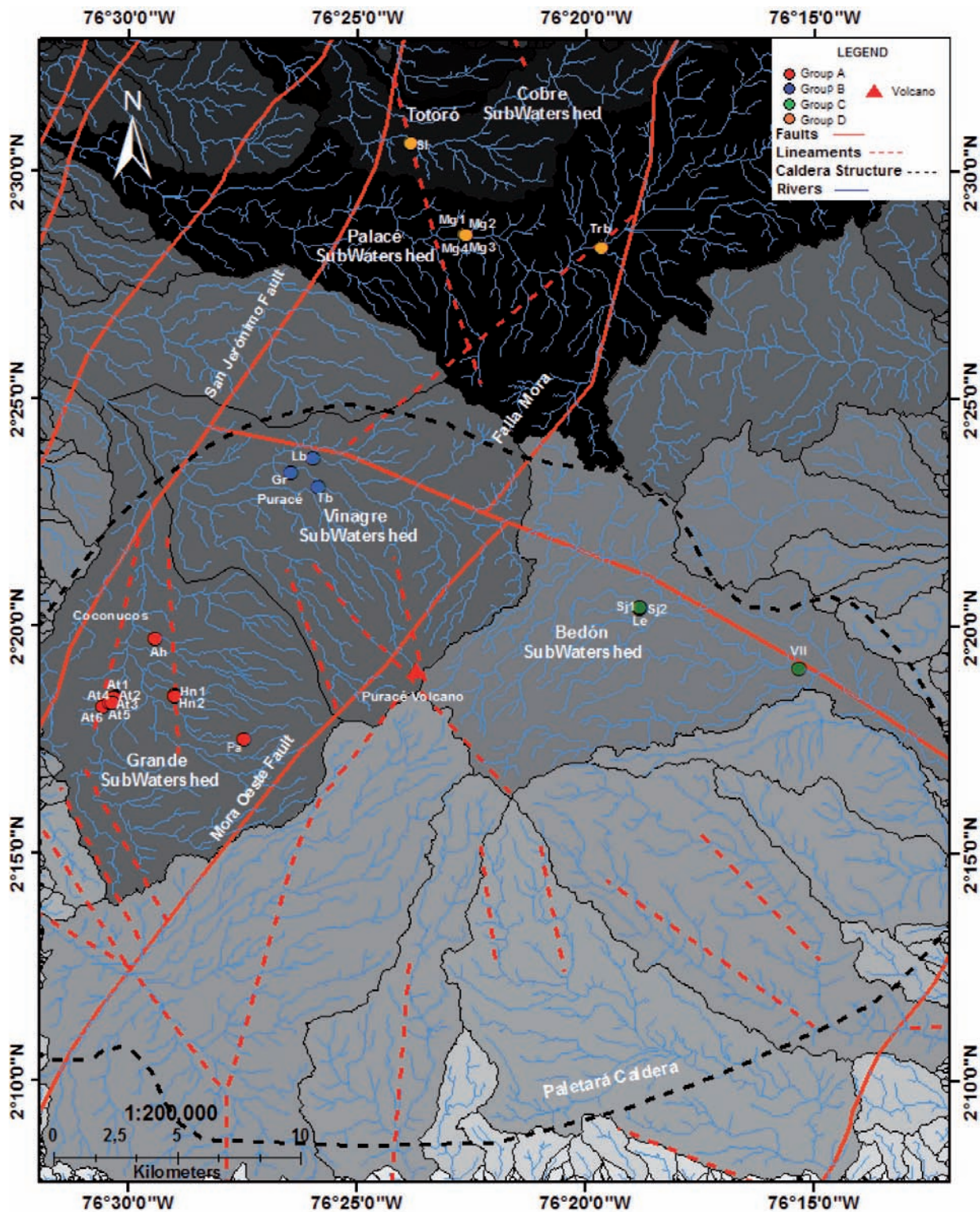


FIGURE 3. Subwatershed delimitation at the PVS with sample locations and geological structures.

## METHODOLOGY

The chemical data of the PVS thermal waters, was obtained from the National Inventory of Hot Springs (2012) summarized by Colombian Geological Survey (CGS), at the website: <http://hidrotermales.sgc.gov.co/>.

The chemical analyses at this site were performed in the CGS at their Water and Gases Laboratory and the Stable Isotopes Laboratory. The analytical techniques included: volumetric analysis, ionic chromatography, UV spectrometry, Atomic Absorption and Inductively Coupled Plasma techniques and for the isotopic analysis Off-Axis ICOS (Integrated Cavity Output Spectroscopy) high-resolution absorption laser spectroscopy. For the interpretation of water chemistry, it is important to know that not all springs will be reliable information about the conditions at depth due to probably either error in the ionic balance or the water is not in equilibrium with the system. Therefore, hot or boiling chloride springs with a strong outflow have experienced the least contamination, so they

are the most suitable for reservoir-related research (Nicholson, 1993).

In order to verify the reliability of the chemical analyzes presented by the GSC, we calculated the Charge Balance Error ion (Equation 1) to identify the ionic imbalances and analytical errors at the time of sample selection. If the results of the Charge Balance Error ion (CBE) exceeds +/- 10% are not suitable for plot and geothermometers (Nicholson, 1993).

For the CBE it was used the following solutes: Sodium (Na<sup>+</sup>), Potassium (K<sup>+</sup>), Calcium (Ca<sup>2+</sup>), Magnesium (Mg<sup>2+</sup>), Lithium (Li<sup>+</sup>), Bicarbonates (HCO<sub>3</sub><sup>-</sup>), Fluorine (F<sup>-</sup>), Sulphate (SO<sub>4</sub><sup>2-</sup>), Chloride (Cl<sup>-</sup>). The compiled data (TABLE 1) shows thermal water chemistry at the PVS.

$$CBE\% = \frac{\sum Cations - \sum Anions}{\sum Cations + \sum Anions} \times 100 \quad (1)$$

It is worth highlighting that the hot spring La Mina was immediately discarded for this study because its pH is very acid (1.73) and it not gives reliable results.

TABLE 1. Chemical analyses of the thermal waters at PVS.

Group A		Mg/L										
Sample	pH	Li	Na	K	Ca	Mg	SiO <sub>2</sub>	B	Cl	F	SO <sub>4</sub>	HCO <sub>3</sub>
At1	6.81	-	53.2	14.4	16.2	11.6	107.36	0.68	13.9	0.34	14.6	272.06
At2	6.82	0.2	166	29	22.5	16.2	127.93	2.15	89.6	0.41	107.86	445.3
At3	6.86	0.45	173	29.2	23	16.05	144.21	2.22	93.9	0.41	109.12	430.66
At4	7.1	4.5	1795	65	76	16	162.64	30.6	1140	1.15	1088	1594.54
At5	6.93	0.2	84.4	20.5	24.2	18	120	0.7	30.96	0.38	31.23	414.8
At6	6.63	0.40	228.00	25.40	28.00	17.40	122.79	3.31	163.50	0.47	150.00	501.41
Ah	6.50	4.00	2340.00	224.00	116.00	38.00	124.71	36.86	1920.00	1.05	2792.00	1395.00
Hn1	3.36	1.8	460	77.9	24	8	234	8.32	433.59	1.29	753.89	-
Hn2	3.38	1.80	547.67	78.05	21.61	36.77	239.36	8.54	438.90	1.24	785.62	-
Pa	2.53	-	13.70	3.45	11.75	4.70	277.07	0.30	2.12	-	590.15	-
Group B		Mg/L										
Tb	2.24	0.10	97.80	23.30	71.50	103.60	122.14	0.70	402.66	-	1222.32	-
Gr	2.54	0.20	80.00	18.00	60.00	79.40	106.71	0.50	220.23	5.41	710.00	-
Lb	2.46	0.20	65.40	12.70	46.60	60.70	105.86	0.40	171.14	5.47	644.15	-
Group C		Mg/L										
Le	4.35	-	59.7	11.05	262	67.2	125.14	0.2	25.82	0.4	1131.88	-
Sj1	4.53	-	60.4	9.5	256	63	97.93	0.25	19.34	0.55	1034.83	-
Sj2	4.70	-	67.60	8.90	288.00	67.60	105.64	-	15.00	0.47	1182.51	-
Vll	6.61	1.00	338.00	25.50	3.20	43.30	145.50	3.20	158.00	-	-	-
Group D		Mg/L										
Sl	6.53	9.00	2640.00	120.00	322.00	118.00	117.64	72.80	2960.00	0.36	578.00	4294.40
Mg1	6.43	4.50	1570.00	100.00	124.00	30.00	129.64	30.00	1558.94	0.58	648.36	2344.84
Mg2	6.43	5.50	1600.00	103.50	124.00	28.00	124.07	31.70	1596.64	0.48	665.45	2371.68
Mg3	6.55	5.5	1605	103.5	116.5	28	122.7	29.2	1250	0.58	770	2381.44
Mg4	6.56	4.50	1605.00	102.00	120.00	28.00	116.36	31.10	1340.00	0.57	707.42	2389.98
Trp	7.12	-	16.50	3.00	9.50	8.50	96.00	-	-	0.37	1.52	195.20

The interpretation of the chemical data and the calculation of Solute geothermometers and ge indicators were performed based on the spreadsheet proposed by Powell and Cumming (2010). The selected graphs and Solute geothermometers were: Tesh, Tclb & Tcfb, Tnkm, Amorphous Silica, chalcedony, quartz via conductive cooling and quartz via adiabatic cooling (boiling).

The Fournier and Potter (1982) quartz geothermometer was chosen over the earlier Fournier (1981) formula, due to its higher temperature range (up to 330°C versus 250°C) (Powell and Cumming, 2010). For the Cation geothermometers, it was calculated the empirical Na-K-Ca geothermometer (Fournier, 1981). Six different versions of the Na/K geothermometer are presented, yielding temperature differences of 20 to 80°C. These are probably not accurate below about 150°C and there are usually commonly greater than the maximum measured temperatures found in drill holes (Powell and Cumming, 2010).

Finally, the K/Mg geothermometer is based on rules by Giggenbach (1988), this geothermometer is valid for

temperatures between 50-300°C, and is most used in the study of low to intermediate equilibrium systems when equilibrium is not reached between the fluid and the complete mineralogical formation of the host rock (Nicholson, 1993). The Silica Geothermometers equations are illustrated in the APPENDIX 1 and the Cation Geothermometers equations in the APPENDIX 2.

## HYDROGEOCHEMISTRY DATASET ANALYSIS

The analysis of the hydro-geochemistry dataset was done for the 4 delimited zones (A, B, C, D) in the PVS. The CBE% estimations, water types at PSV and geothermometers are presented in this section.

### Charge Balance Error (CBE%)

The CBE estimations (TABLE 2) indicate that zone B is reflecting an imbalance in the samples probably due to problems of collection of the sample or by endogenous processes in the system. Therefore, this zone was discarded and not used for the geothermometers analysis.

TABLE 2. Calculation of CBE% of thermal waters at PVS.

Group A						
Hot springs	Sample	pH	Temp °C	∑Cations	∑Anions	CBE%
Agua Tibia 1	At1	6.81	23.8	4.445157	5.173052	-8%
Agua Tibia 2	At2	6.82	28	10.446864	12.093310	-7%
Agua Tibia 3	At3	6.86	37	10.805103	12.000897	-5%
Agua Tibia 4	At4	7.1	31	85.501683	81.006606	3%
Agua Tibia 5	At5	6.93	30.30	6.912783	8.342165	-9%
Agua Tibia 6	At6	6.63	33	13.453878	15.978185	-9%
Agua Hirviendo	Ah	6.50	74.10	117.008714	135.211962	-7%
Hornos 1	Hn1	3.36	70	24.550004	27.995469	-7%
Hornos 2	Hn2	3.38	67.50	30.595355	28.803251	3%
Pozo Azul	Pa	2.53	88.30	4.584713	12.346728	-46%
Group B						
Tabio	Tb	2.24	22	22.662842	36.807741	-24%
Guarquello	Gr	2.54	23.20	16.355485	21.279670	-13%
La Bajada	Lb	2.46	23.20	13.956612	18.527003	-14%
Group C						
Laguna Esmeralda	Le	4.35	33.5	21.525481	24.315179	-6%
San Juan1	Sj1	4.53	33	20.856371	22.119694	-3%
San Juan2	Sj2	4.70	34.30	23.119942	25.067749	-4%
Versalles	Vll	6.61	34.80	19.220926	26.243679	-15%
Group D						
El Salado	Sl	6.53	24.10	144.980163	165.939726	-7%
Mangas 1	Mg1	6.43	46.30	80.156263	95.939011	-9%
Mangas 2	Mg2	6.43	48	81.530348	97.792985	-9%
Mangas 3	Mg3	6.55	53.7	81.373509	90.356232	-5%
Mangas 4	Mg4	6.56	52.90	81.365688	91.731661	-6%
Trampa	Trp	7.12	25.20	1.967795	3.250451	-25%



### Classification of waters

The classification of the PVS water types was classified through major anion concentrations making the Tsch plot and it is summarized in TABLE 3.

In the Tc1b Plot (FIGURE 4A) is possible to observe concentrations relatively low in lithium with a high relation between Cl/B where the group A and D present similar amounts having a similar tendency,

while the group C presents quantities of lithium below the limit of quantification of lithium and less amount of Cl reflecting in Cl/B. The Tc2b Plot (FIGURE 4B), shows a behavior similar to the last plot but in this case F/Cl ratio is relatively similar between group A and D, but group C again shows a behavior different from the other groups. Ratios of chloride, boron and lithium may be used to track common sources in a reservoir.

TABLE 3. Water types summary at the PSV.

Group	Water type	Occurrence	Applicable geothermometers
A	Sulphate-chloride to bicarbonate	Mixing of chloride and sulphate water at variable depth. The changes Sulphate-chloride: it is possible to bicarbonate water type may relate to apply with caution because ate to be the product of steam and gas mixed fluids.	condensation into poorly oxygenated Bicarbonate: not doubtful for sub-surface groundwater's. They are geothermometers common at the margin of the fields.
C	Acid-sulphate waters	Superficial fluids formed by the condensation of geothermal gases into near-surface. oxygenated groundwater.	Doubtful for geothermometers, because the concentration of silica and most cations are the product of near-surface leaching.
D	Dilute chloride - bicarbonate	These waters are formed by the dilution If the chloride waters are only of chloride fluid by either ground water being diluted by ground water, then or a bicarbonate water during later flow. geothermometry may be applicable.	

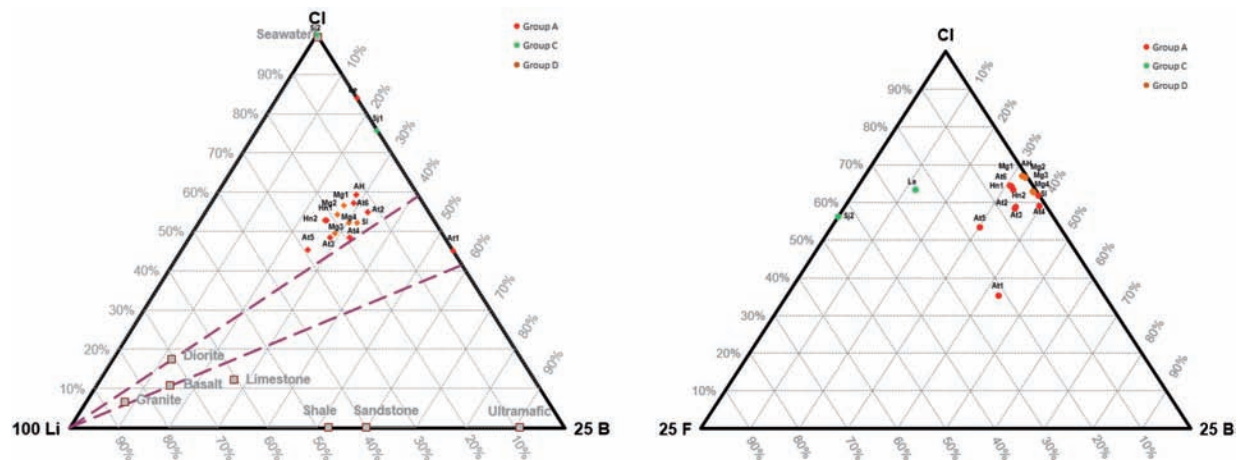


FIGURE 4. A. Tc1b Plot. B. Tc2b Plot; Group A red dots, Group C green dots and Group D orange dots. The plots were made on using the spreadsheet of Liquid Analysis v3 (Powell and Cumming, 2010).

The Tnkm plot reveals that group A presents partial equilibrium springs (FIGURE 5), which are springs Ah and At4, in addition to the other emanations, there is no equilibrium, but there is a slight tendency towards the 220°C line. According to the plot, the group A springs plot between 160°C - 225°C. The group D, the

springs present temperatures in the range of 180°C - 200°C. The group C shows immature waters and is not possible to observe a trend suggesting that this group may not be ideal for geothermometers specially Na/K geothermometers.

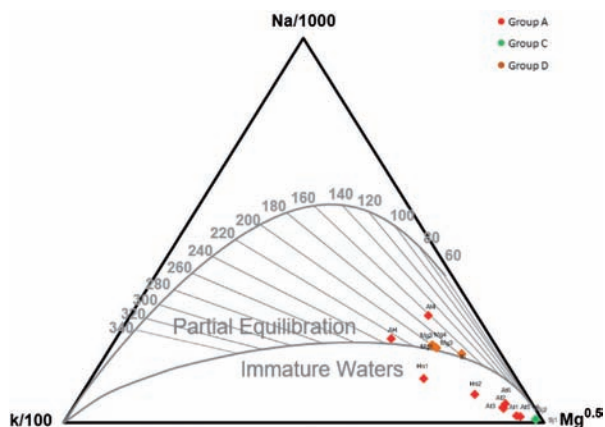


FIGURE 5. Tnkm Plot; Group A represented by red dots, Group C green dots and Group D orange dots. The plot was made on spreadsheet of Liquid Analysis v3 (Powell and Cumming, 2010).

### Solutes geothermometers

The calculated values for Solute geothermometers in the PVS are summarized in TABLES 4 and 5.

Values on TABLE 4 were calculated with Silica geothermometer. These geothermometers work with the solubility of different silica species in water as a function of temperature and pressure (Karingithi, 2009). The Quartz geothermometers are suitable for temperatures >150°C, below this temperature, the Chalcedony and α-Cristobalite geothermometer that goes between 100°C - 150°C and below 100°C for Amorphous Silica is recommended. It was discarded the Amorphous Silica and β-Cristobalite because the temperature of Amorphous Silica is similar to the discharge temperature and β-Cristobalite is stable at very high temperatures and is probably not in the system. These values can be overestimated or underestimated depending on the conditions that the reservoir is found on, and later the appropriate ones for the study of the waters must be chosen. All the geothermal units are added for each group to know the temperature differences when they do not meet the requirements, although later those that are unsuitable will be discarded.

TABLE 4. Value of Silica Geothermometers in °C (See APPENDIX 1 for the used equations).

Group	Sample	Alpha Cristobalite	Chalcedony conductive	Quartz conductive	Quartz adiabatic
A	At1	91	115	141	136
	At2	101	126	152	145
	At3	108	135	159	151
	At4	116	143	167	157
	At5	97	122	148	141
	At6	98	124	149	143
	Ah	99	125	150	143
	Hn1	142	172	192	177
	Hn2	143	173	193	178
C	Le	100	125	150	144
	Sj1	85	109	136	132
	Sj2	90	114	140	135
D	Sl	96	121	147	140
	Mg1	102	127	152	145
	Mg2	99	124	150	143
	Mg3	98	124	149	143
	Mg4	95	120	146	140

As mentioned above, the Cation geothermometers depend on the temperature of the ion exchange or partitioning of alkalis between the solutions and the solid. TABLE 5 shows different Cation geothermometers where four different versions of the Na/K geothermometer are presented, since they are proposed by several authors with varying temperatures of 20°C to 50°C approximately. The Na/K geothermometers work well for reservoirs with

temperatures between 180°C - 350°C, however at lower temperatures they lose their usefulness. In this case, the K/Mg geothermometer is suitable under 150°C and the Na-K-Ca and Mg correction is suitable in temperatures above 100°C. Na-K-Ca geothermometer shows a good correlation with mature waters shown in the Tnkm plot. The values of Silica and Cation geothermometers were taken into account in both tables regardless of whether they were suitable or not for analysis between them.

**TABLE 5.** Value of Cation Geothermometers in °C; (1) Fournier and Truesdell, 1973, (2) Fournier, 1979, (3) Fournier, 1979, (4) Truesdell, 1976, (5) Giggenbach, 1988, (6), Tonani, 1980, (7) Giggenbach, 1988 (See APPENDIX 2 for the used equations).

Group	Sample	Na-K-Ca (1)	Na-K-Ca Mg corr. (2)	Na/K (3)	Na/K (4)	Na/K (5)	Na/K (6)	K/Mg (7)
	At1	111	31	320	327	327	382	74
	At2	211	32	270	257	281	301	87
	At3	210	33	266	252	278	296	88
	At4	157	87	143	99	162	124	109
A	At5	217	25	307	308	315	360	77
	At6	189	30	226	199	241	236	83
	Ah	212	90	213	183	229	218	134
	Hn1	230	116	267	252	278	296	125
	Hn2	224	21	249	229	262	270	103
	Le	44	44	276	265	287	311	49
C	Sj1	41	41	259	242	271	285	47
	Sj2	38	38	242	219	255	259	45
	Sl	163	45	158	116	176	143	99
	Mg1	180	80	181	144	199	174	113
D	Mg2	181	86	182	145	200	175	115
	Mg3	181	83	182	145	200	175	115
	Mg4	180	84	181	143	199	174	114

## DISCUSSIONS

### Hydrogeochemical process

The chemistry of the waters at the PVS, indicated that Group B presents an imbalance (e.g. CBE exceeds +/- 10%), causing the entire group to be discarded for different analysis. This error in the ionic balance may be due to an error during the collection of sample or probably due to high acidity in the waters. Other springs of group A, C and D was also discarded for the same reason.

Considering the Tsch plot (FIGURE 6), the group A waters present a variation between bicarbonate waters to chloride-sulphate waters that can be caused by the different distance to the volcano crater since the farther areas present waters enriched with bicarbonate, while the waters near the volcano are enriched in sulfates and chlorides.

The  $\text{HCO}_3$  can be derived either by the dissolution of  $\text{CO}_2$  or by condensation of relatively deep oxygen-free groundwater geothermal steam, while the gains in  $\text{SO}_4$  is related to magmatic gases that rise through

the permeable zones. The Group C waters are acid sulphates; the reason for the absence of the  $\text{HCO}_3$  may be possibly for the topographic levels, since the springs are above the water table or there is absence of  $\text{CO}_2$  in vapor, this absence may be originated during ascent of spring to the surface, fluids can experience  $\text{CO}_2$  losses by a phase separation and loss of vapor resulted of the mineral precipitations such as the calcite (Giggenbach, 1993). In this group, it can be deduced that the composition is dominated by steam condensation into near surface waters causing high concentrations of sulphate and calcium (Nicholson, 1993) and this explains the low amounts of remaining dissolved solids. Although Group D waters plots are located at the apex of bicarbonate water, they present high amounts of  $\text{Cl}^-$  and  $\text{Na}^+$  with a pH close to neutrality showing a tendency towards maturity, coming from a zone of water partially balanced in the fluid - rock interaction. Moreover, they contain larger amounts in elements than the other groups. These higher concentrations could be related the interaction with hot waters, acidic magmatic gases and favorable conditions for the leaching of major rock forming cations and anions from host rock formations.

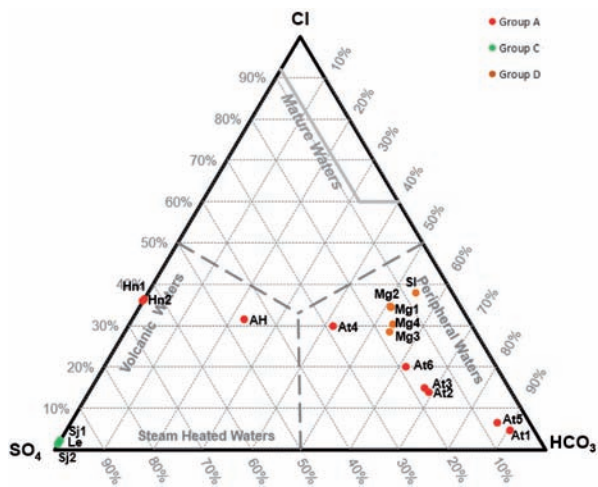


FIGURE 6. Tcsh Plot; Group A are represented by red dots, Group C green dots and Group D orange dots. The plot was made on spreadsheet of Liquid Analysis v3 (Powell and Cumming, 2010).

On the other hand, on the TcIb Plots (FIGURE 5) is possible to observe a loss of lithium and a relation between Cl/B possibly indicating vapor absorption by magmatic gases in groups A and D. Furthermore, in the TcIb Plot a relation of fluoride similar in these two groups suggests that they are probably related to the same upflow. Moreover, the relation between Cl/B and Cl/Li ratios has a strong positive correlation possibly indicating a common source for the groups A and D (FIGURE 7). Li and B concentrations are significantly higher in the group D than in the group A. If it supposes they are the same upflow, the mineral alteration reactions near surface can remove these elements in the case of group A or this can be attributed to changes in lithology and the adsorption of B and Li into clays during lateral flow by leaching out of the host rock.

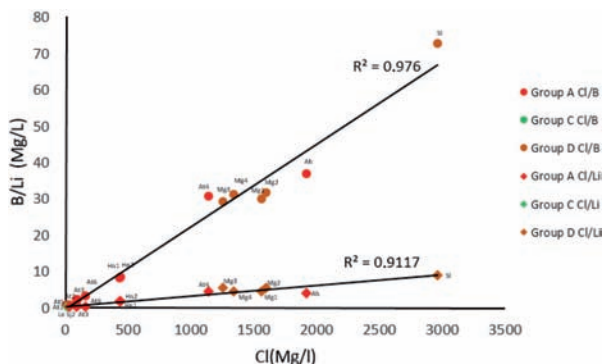


FIGURE 7. Cl/B and Cl/Li ratios for Puracé hot springs. The R<sup>2</sup> values for both ratios are around 0.9 indicating a good fit of the model to the data.

This is probably due to higher reservoir temperatures closer to the surface where the flow increases the

amounts of B and Li among other elements. The anomaly fluoride group At4 may occur when volcanic gases (HF) are condensed into meteoric waters and accompany high levels of Cl and SO<sub>4</sub> (Nicholson, 1993) where the other At springs do not show this particularity. The group C presents a low Cl/B ratio, being very sulfated waters can be understood as a direct relation in the absorption of magmatic gases or condensation, and it shows differences in the amount of fluoride and absence of lithium showing that they are possibly of a different upflow.

In group A, the Ah and At4 along with all the springs of group D present partial equilibrium as can be seen in the Tnkm plot (FIGURE 5), but the springs of group C do not present such balance. On the plot it is possible to observe that group A shows a tendency to 220° group C although the spring At4 indicates a minimum of 160°C inferring that the range in this zone is between 160°C - 225°C, while group D shows a range between 180°C - 200°C.

Solute geothermometers are based on temperature-dependent mineral-fluid equilibrium and their successful application needs to be applied only to those spring samples with the suitable characteristics for geothermometer applications. Therefore, were chosen the spring waters from groups A and D with the highest temperature and chloride concentrations based on the Cl-HCO<sub>3</sub>-SO<sub>4</sub> water classification diagram and K-Na-Mg plot. However, the springs of Hornos should be discarded for geothermometers due to their acidity where rocks can be leached very close to the surface and determines overestimated values, they could be taken into account with caution since they do not present great changes in addition of cations. Using the geothermometers of Silica, for group A, the Quartz Conductive and Chalcedony geothermometers were chosen, except for Agua Hirviendo, Hornos 1 and 2 where it was Adiabatic Quartz was chosen instead for its characteristics of perspiring vapor, where the geothermometer indicates temperatures of >140°C. Group A generally presents values between 120°C to 150°C considering as well as geothermometers in the group D. While, the Cation geothermometers present varying values from less than 100°C to almost 300°C, the difference between them could be either due to the amounts in cations used for calculating the geothermometer (overestimating or underestimating temperatures) or two phases of mineral equilibrium as seen in the K/Mg geothermometers. It is possible that the phase of equilibrium in low temperature is determined by the K/Mg geothermometers while the other phase of higher temperature is determined by

Na/K and Na-K-Ca geothermometers. Nevertheless, the Na/K geothermometers were not taken into account for waters that were not in partial equilibrium shown in the Tnkm plot, because they are immature waters. This range of higher temperatures presents values >180°C in group A except in the spring At4 where the temperature calculated for the Na-K-Ca geothermometer is very similar to Tnkm plot which is in a partial equilibrium increasing confidence. In the case of group D the values that correlate with Tnkm plot were chosen in order to have higher reliability such as Na-K-Ca and Na/K Giggenbach geothermometers that indicate temperatures between 170°C - 200°C. The Na-K-Ca with corrected Mg geothermometer was discarded. Apparently, there is a mixture with surface waters evidenced in the ion analysis making unsuitable the use of this geothermometer. The difference in the range between the silica and cation geothermometers is due to the tendency of Cation geothermometers to estimate higher temperatures because it rebalances faster, so it is useful to estimate temperatures at a greater depth of the system. Also, the Silica geothermometers may be lower due to the presence of high salinity fluids that alter quartz solubility and change the pH for shallow mixing with cold meteoritic water.

To analyze the mineral phases in equilibrium in low temperature, two geoindicators are used which are Xkms and Xkmc diagrams. The Xkms diagram (FIGURE 8A) shows a range with temperatures varying between ~80°C to ~130°C for groups A and D. They are plotted on the Quartz (conductive), Chalcedony or Alpha Cristobalite solubility line. Using this geoindicator helps comparing two low temperature geothermometers, increasing confidence in both if they match. On the other hand, the Xkmc diagram (FIGURE 8B) helps understand the processes based on equilibrium between K-feldspar, calcite and K-mica on one side and dissolved Ca<sup>+2</sup> and K<sup>+</sup> on the other to determine the partial pressure of CO<sub>2</sub> at the final temperature of the water equilibration with rock, as determined by the K-Mg geothermometer where the values that are below the equilibrium line have the CO<sub>2</sub> pressure (PCO<sub>2</sub>) higher than full equilibrium PCO<sub>2</sub> and can promote Ca-Al silicates to calcite and possibly explain a possible formation of some clay minerals. These diagrams corroborate Na/K geothermometers corresponds to deep equilibrium conditions at the highest temperature, whereas K/Mg geothermometer represents shallower equilibrium conditions at the lowest temperature.

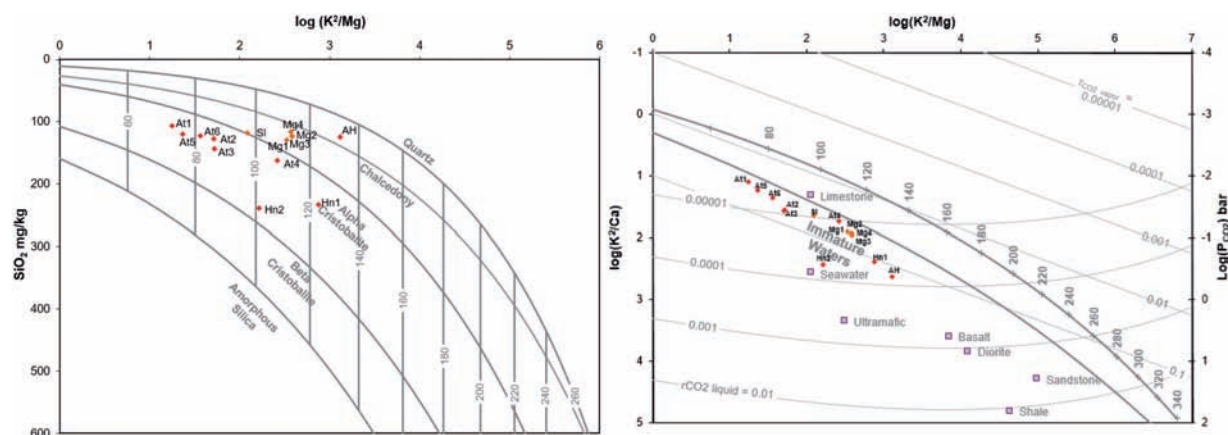


FIGURE 8. A. Xkms diagram and B. Xkmc diagram; Group A represented by red dots and Group D orange dots. The diagrams were made on the spreadsheet of Liquid Analysis v3 (Powell and Cumming, 2010).

### Evaluation of mixing processes

To understand if there is a mixture of different types of water, using the graph proposed by Giggenbach (1992) it is possible to see the stable isotopes to establish the origin of discharged fluids, sub-surface water mixing, water-rock interaction, and vapor separation processes (Nutti, 1991). In this case the isotope δ18O and 2H is used to know the origin of the waters. The applications of water isotopes are also useful in characterizing the

boiling process and in monitoring flow of injected fluids (Arnórsson, 2000).

The red line is the segment of the Colombian Meteoric Line (CML) and the gray line is Global Meteoric Water line (FIGURE 9). The thermal waters of the study area are very close to the GWML and CML lines, however, they have a notorious δ18O slanting, showing a possible mixing of hydromagmatic fluids. This behavior can be seen in both groups A and D. The lower rectangle is

a close up that shows where steam water equilibrium fractionation of groups A and D present a linear regression indicating a temperature above 250°C for

group A and 160°C for group D exhibiting similitude with high temperature geothermometers.

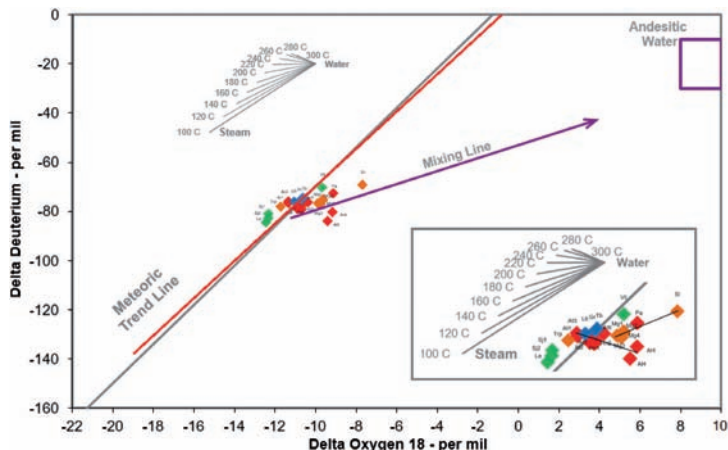


**FIGURE 9.** Cross-plot of the stable isotopes of water ( $\delta^{18}\text{O} - \delta\text{D}$ ). It includes the World Meteoric Trend line, the range of andesitic water as proposed by Giggenbach (1992). Group A thermal waters are represented by red dots, Group B thermal waters blue dots, Group C thermal waters green dots and Group D thermal waters orange dots. The cross-plot was made on the spreadsheet of Liquid Analysis v3 (Powell and Cumming, 2010).

Another way of evaluating the mixture is through a linear relation of Cl with  $\delta^{18}\text{O}$ , Na and B. These linear relations evidence that ascending hot water has mixed with cold water. According to Arnórsson and Gunnlaugsson (1985) a positive relationship between that Cl and  $\delta^{18}\text{O}$  relation reveal evidence of mixing (Arnórsson and Gunnlaugsson, 1985) and other authors

such as Burgos (1999) argues the linear relation between chloride and boron and chloride and sodium show evidence of mixing. In the FIGURE 10 illustrate a positive relationship between Cl with  $\delta^{18}\text{O}$  (FIGURE 10A), Cl – Na (FIGURE 10B) and Cl - B (FIGURE 10C) suggesting a dominance of the mixing process, making most reliable the data about the stable isotopes diagram.

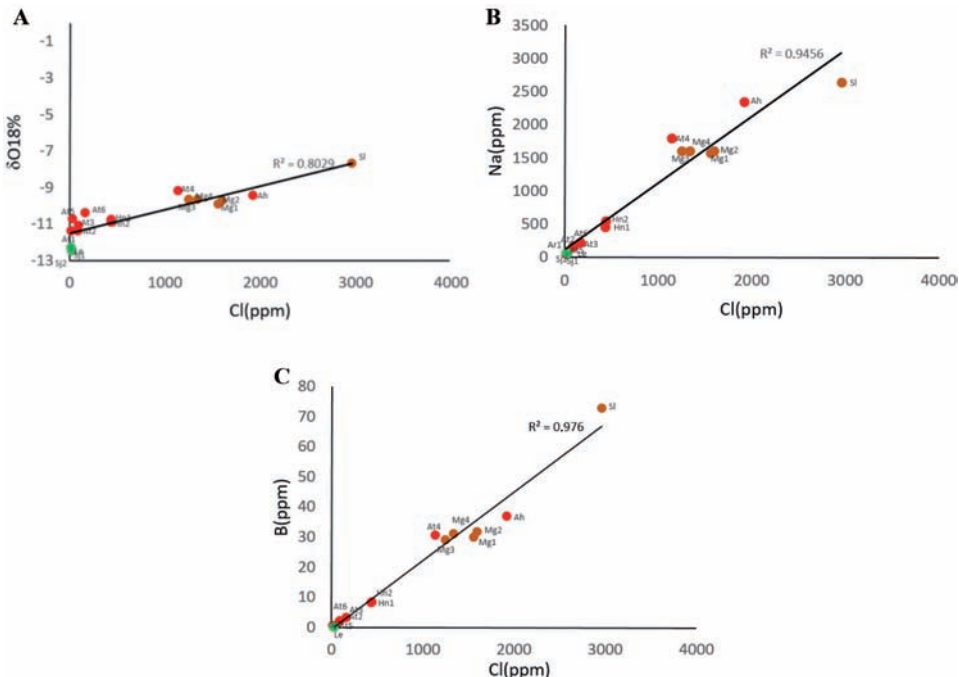


**FIGURE 10.** A. Cl vs  $\delta^{18}\text{O}$  diagram. B. Cl vs Na diagram. C. Cl vs B diagram. Group A represented by red dots, Group B blue dots, Group C green dots and Group D orange dots. The  $R^2$  values with ratios around 0.9 indicating a good fit of the model to the data.

### Preliminary conceptual model

The preliminary conceptual model of the geothermal system in the survey zone is shown in FIGURE 11 and FIGURE 12. It suggests that the heat source in the geothermal system could probably be related to PVS where a transtensional fault allows the magma to ascend to close to surface. Therefore, it seems that the fluid flow of the geothermal system is controlled by permeable zones associated to faults, which play an important role in vertical permeability of geothermal systems. The seal rocks might be represented by impermeable volcanoclastic rocks from the Quaternary with Pliocene rocks. The reservoir should correspond to ignimbrites and other volcanoclastic rocks along with rocks from the Cajamarca complex suggesting a fracture zone influenced at the same time by the schistosity where the hot water fluids accumulate. The

geological structures and the distribution of thermal manifestations on surface also indicate that the fluid flow is controlled by faults. The relative concentration of conservative ions and the B/Cl suggests different upflow for Group A and C but same plow for group A and D. The study of the isotopic composition of  $\delta 2H$  vs  $\delta 18O$ , as well as the linear relation of Cl with  $\delta 18O$ , Na and B in the hot springs, indicates that waters in the geothermal reservoir are originated from the mixing of meteoric waters with geothermal fluids. Considering that group A presents the best area for geothermal exploration due to the temperature of its geothermometers and geological characteristics, it can be assumed that the area of the minimum temperature reservoir is located around the hot springs of Aguas Tibias and the maximum is near the area Agua Hirviendo and Hornos.

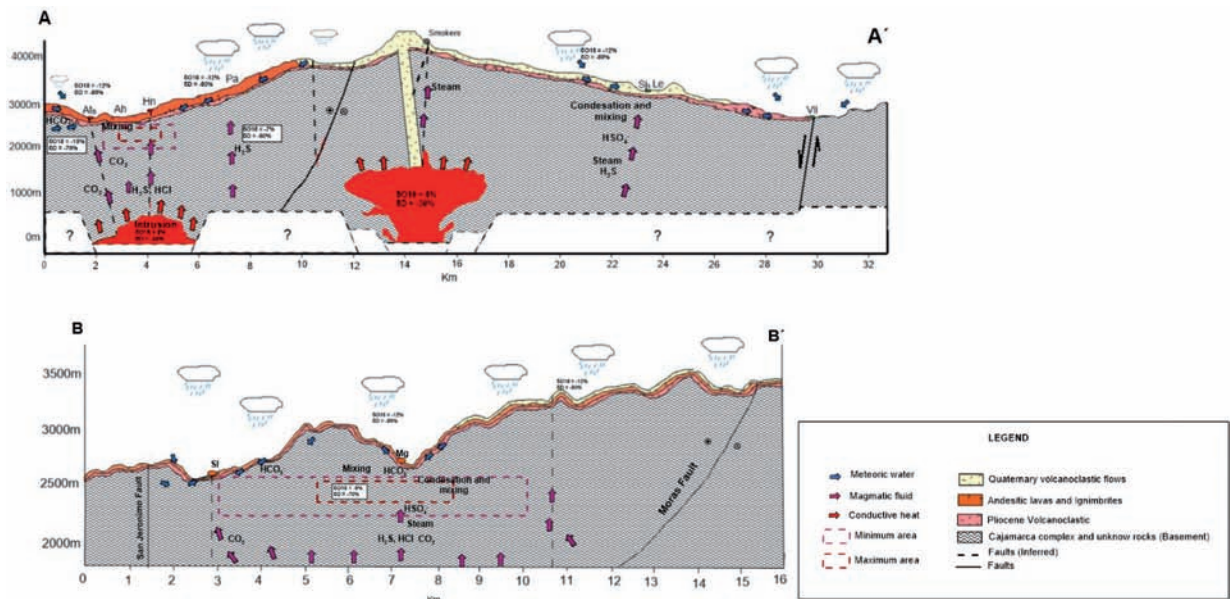


FIGURE 11. **A.** Preliminary conceptual model of Puracé system, the springs Ah, Pa, Sjl, Sj2 and Le are the projection about the line section. **B.** Preliminary conceptual model of Puracé system. See localization of both Cross-section in the FIGURE 12.

The map of potential areas (FIGURE 12) was done based on the probability of increased porosity by a structural control under the subsoil as it can be an intersection of faults due to the adjacent regional faults

in the system together with the tendency of the waters towards the maturity and enrichment of  $\delta 2H$  vs  $\delta 18O$ , with a high-enthalpy system (Group A) and low-enthalpy to high enthalpy system (Group C).

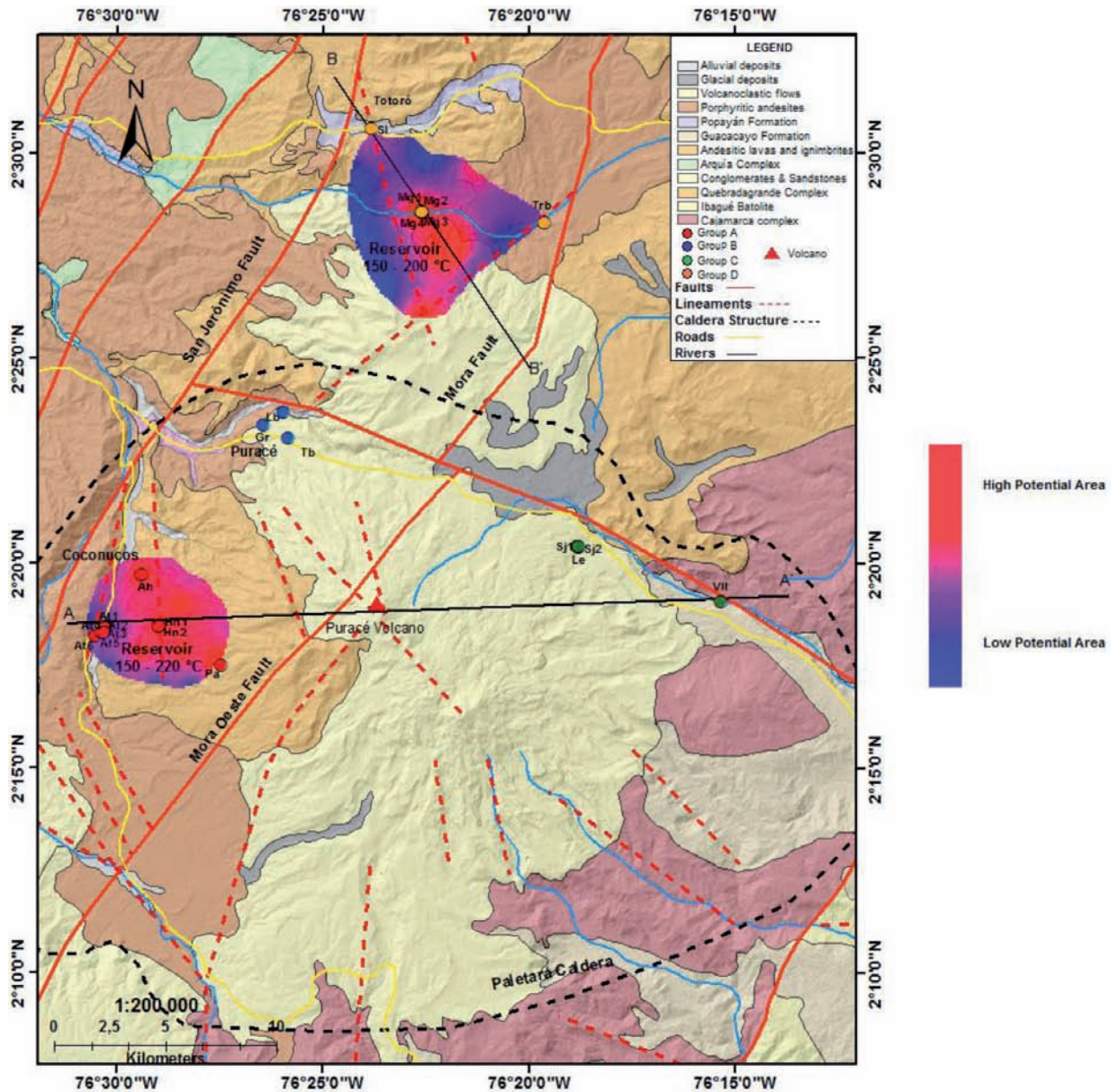


FIGURE 12. The PVS geothermal potential areas were determined by geology, inferred faults, geothermometers and geoindicators of the thermal springs.

## CONCLUSIONS

The study area presents an important water recharge possibly due to its large number of drainage systems along with the Cauca River, which can contribute to infiltration of the waters to reservoir rocks. Also, the structural control plays an important role for the infiltration of the waters because it generates secondary porosity in rocks in less porous rocks. Several springs are in the lineaments that were originated by the lateral movement of regional faults, allowing these emanations.

The geochemical characterizations of the thermal springs at PSV are summarized as follows:

- Four water groups have been selected, where all hot springs in-group B were discarded for not being suitable to have a very high charge balance error (>10%).
- The water types at PSV are: Bicarbonate (Group A: At1, At2, At3, At5), dilute chloride (all Group D and group A: t4), acid-sulphate (all Group C, B) and sulphate-chloride (Group A: Hn1, Hn2, Ah) and Heated steam-acid sulfated (Group A: Pa) waters.



- The conservative elements plots (B, Cl, F, Li) allow inferring the upflow of group A and grouping D probably are the same and the group C is different to them.
- The correlation of Tnkm plot with geothermometers allows inferring that the temperature of the reservoir in-group A ranges between 150°C - 220°C and in-group D between 150°C - 200°C. However, in groups B and C it was not possible to determine the temperature since they didn't have appropriate conditions to be calculated.
- The correlation between some geothermometers and geoindicators indicate a possible mineral equilibrium phase in low temperature (~100°C). However, there is another mineral equilibrium phase in temperatures >150°C estimated through geothermometers used in high temperatures.
- Mixing processes between geothermal fluids with meteoric waters have been identified through isotopic analyses and different relationships with chloride.

Knowing the above-mentioned characteristics, it is evident that meteoric waters that infiltrated through the fractures and faults recharge the hot springs at the PVS. The study area presents a potential zone of high – enthalpy to the west of PVS, around the Hornos and Agua Hirviendo springs and another zone to the north indicating high- enthalpy resource around Mangas springs both associated to fault system with magmatic activity.

## ACKNOWLEDGEMENTS

We thank the Research Direction at EAFIT University, for its economic support to the geothermal research project inside of the Regional Geology and Geochemistry research seedlings. Special thanks to the members of the research seeding and to Ana M. Contreras for her support during the development of this research and to Colombian Geological Survey (CGS) for share physical chemical data of thermal waters through National Inventory of Thermal Waters.

## REFERENCES

- Arnórsson, S. (2000). *Isotopic and chemical techniques in geothermal exploration, development and use. Sampling methods, data handling, interpretation*. Vienna: International Atomic Energy Agency.
- Arnórsson, S., and Gunnlaugsson, E. (1985). New gas geothermometers for geothermal exploration-calibration and application. *Geochimica et Cosmochimica Acta*, 49(6), 1307-1325. doi: 10.1016/0016-7037(85)90283-2.
- Bohorquez, O.P., Monsalve, M.L., Velandia, F., Gil, F., y Mora, H. (2005). Marco tectónico de la cadena volcánica más septentrional de la cordillera central de Colombia: *Boletín de Geología*, 27(44), 55-79.
- Burgos, M. (1999). Geochemical interpretation of thermal fluid discharge from wells and springs in Berlin geothermal field, El Salvador. *Geothermal Training Programme*, Report Number 7, Reykjavík, Iceland.
- Chandrasekharam, D., and Bundschuh, J. (2008). *Low-enthalpy geothermal resources for power generation*. Leiden: CRC Press/Balkema.
- Ellis, A.J., and Mahon, W.A.J. (1977). *Chemistry and geothermal systems*. New York: Academic Press INC.
- Fournier, R.O. (1979). A revised equation for the Na/K geothermometer. *Geothermal Resources Council Transactions*, 5, 1-16.
- Fournier, R.O. (1981). Application of water geochemistry to geothermal exploration and reservoir engineering. In L. Ryback, and L.J.P. Muffler (Eds.), *Geothermal systems: Principles and case histories* (pp. 109-143). Chichester: John Wiley and Sons.
- Fournier, R.O., and Potter, R.W. (1982). A revised and expanded Silica (Quartz) geothermometer. *Geothermal Resources Council Bulletin*, 11(10), 3-12.
- Fournier, R.O., and Truesdell, A. (1973). An empirical Na–K–Ca geothermometers for natural waters. *Geochimica et Cosmochimica Acta*, 37(5), 1255-1275. doi: 10.1016/0016-7037(73)90060-4.
- Garzón, G., Salazar, S.P., Serna, D.Y., Bobadilla, L., Lesmes, L.E., Diago, J.C., and Mojica, J. (2004). Thermal springs of Colombia active volcanoes. *11th International Symposium on Water-Rock Interaction*, Londres.

- Giggenbach, W.F. (1988). Geothermal solute equilibria. Derivation of Na-K-Mg-Ca geothermometers. *Geochimica et Cosmochimica Acta*, 52(12), 2749-2765. doi: 10.1016/0016-7037(88)90143-3.
- Giggenbach, W.F. (1991). Chemical techniques in geothermal exploration. In: F. D'Amore (Ed.), *Applications of geochemistry in geothermal reservoir development* (pp. 119-144). Roma: UNITAR.
- Giggenbach, W.F. (1992). Isotopic shifts in waters from geothermal and volcanic systems along convergent plate boundaries and their origin. *Earth and Planetary Science Letters*, 113(4), 495-510. doi: 10.1016/0012-821X(92)90127-H.
- Giggenbach, W.F. (1993). Redox control of gas compositions in Phillipine volcanic hydrothermal systems. *Geothermics*, 22(5-6), 575-587. doi: 10.1016/0375-6505(93)90037-N.
- Giggenbach, W.F., and Goguel, R.L. (1989). *Collection and analysis of geothermal and volcanic water and gas discharges*. 4th Ed. Report No. CD 2401. Pentone: Department of Scientific and Industrial Research.
- Karingithi, C.W. (2009). Chemical geothermometers for geothermal exploration. *Short Course IV on Exploration for Geothermal Resources*, organized by UNU-GTP, KenGen and GDC, at Lake Naivasha, Kenya, 1-22.
- Marquínez, G., Rodríguez, Y., Terraza, R., y Martínez M. (2003). *Geología de la plancha 365 Coconucos, escala 1:100.000*. INGEOMINAS.
- Maya, M. y González, H. (1995). Unidades litodémicas en la Cordillera Central de Colombia. *Boletín geológico INGEOMINAS*, 35, 43-53.
- Monsalve, M.L. (2000). *Catálogo de las volcánicas Neógenas de Colombia, Fascículo Formación Coconucos*. INGEOMINAS, 32 p.
- Nicholson, K. (1993). *Geothermal fluids: Chemistry and exploration techniques*. Berlin: Springer.
- Nuti, S. (1991). Isotopic techniques in geothermal studies. In: F. D'Amore (Ed.) *Applications of geochemistry in geothermal reservoir development* (pp. 215-250). Rome, Italy: UNITAR/UNDP Centre on Small Energy Resources.
- O'Brien, J. (2010). *Hydrogeochemical characterization of the Ngatamariki geothermal field and a comparison with the Orakei Korako thermal area, Taupo Volcanic Zone, New Zealand*. M.Sc. Thesis. University of Canterbury. New Zealand.
- Powell, T., and Cumming, W. (2010). Spreadsheets for geothermal water and gas geochemistry. *Proceedings of 35th Workshop on Geothermal Reservoir Engineering*. Stanford University, California.
- Servicio Geológico Colombiano. (2012). *INVTERMALES. Inventario Nacional de Manifestaciones Hidrotermales*. Consultado el 20 de febrero de 2017. <http://hidrotermales.sgc.gov.co/>.
- Torres, M.P., Monsalve, M.L., Pulgarín, B., y Cepeda, H. (1999). Caldera de Paletará: Aproximación a la fuente de las ignimbritas del Cauca y Huila. *Boletín Geológico de INGEOMINAS*, 37, 1-15.
- Tonani, F. (1980). Some remarks on the application of geochemical techniques in geothermal exploration. *Proceedings, Advances in European Geothermal Research, 2nd Symposium*. Strasbourg, France.
- Truesdell, A. (1976). Summary of section III: Geochemical techniques in exploration. *Proceedings 2nd United Nations Symposium on the Development and Use of Geothermal Resources*. San Francisco, USA.

---

---

Esteban Gómez-Díaz  
ORCID: 0000-0002-1209-8768

Maria Isabel Marin-Cerón  
ORCID: 0000-0001-9814-8414

---

---

Trabajo recibido: mayo 19 de 2017  
Trabajo aceptado: octubre 25 de 2017

## APPENDIX 1

Silica Geothermometers	
Quartz Adiabatic <b>Fournier and Potter, 1982</b>	$T^{\circ}C = \frac{1522}{5.75 - \text{Log}(\text{SiO}_2)} - 273.1$
Quartz Conductive <b>Fournier and Potter, 1982</b>	$T^{\circ}C = \frac{1309}{5.19 - \text{Log}(\text{SiO}_2)} - 273.15$
Chalcedony <b>Fournier and Potter, 1982</b>	$T^{\circ}C = \frac{1032}{4.69 - \text{Log}(\text{SiO}_2)} - 273.15$
Alpha Cristobalite <b>Fournier and Potter, 1982</b>	$T^{\circ}C = \frac{1000}{4.78 - \text{Log}(\text{SiO}_2)} - 273.15$

## APPENDIX 2

Cation Geothermometers	
Na-K-Ca <b>Fournier and Truesdell, 1973</b>	$T^{\circ}C = \frac{1647}{\text{Log}(\text{Na}/\text{K}) + \beta \text{Log}\left(\frac{\sqrt{\text{Ca}}}{\text{Na}}\right) + 2.24} - 273.15$ ( $<100^{\circ}C$ if $\beta = 4/3$ and $>100^{\circ}C$ if $\beta = 1/3$ )
Na-K-Ca Mg. Correct. <b>Fournier, 1979</b>	Correction T.Na-K-Ca - T $\Delta$ Mg (Temp. Na-K-Ca $>70^{\circ}C$ and R $<50$ ) (No mixing water)
Na/K <b>Fournier, 1979</b>	$T^{\circ}C = \frac{1217}{1.438 + \text{Log}\left(\frac{\text{Na}}{\text{K}}\right)} - 273.15$
Na/K <b>Truesdell, 1976</b>	$T^{\circ}C = \frac{855.6}{0.8573 + \text{Log}\left(\frac{\text{Na}}{\text{K}}\right)} - 273.15$
Na/K <b>Giggenbach, 1988</b>	$T^{\circ}C = \frac{1390}{1.75 + \text{Log}\left(\frac{\text{Na}}{\text{K}}\right)} - 273.15$
Na/K <b>Tonani, 1980</b>	$T^{\circ}C = \frac{883}{0.78 + \text{Log}\left(\frac{\text{Na}}{\text{K}}\right)} - 273.15$
K/Mg <b>Giggenbach, 1988</b>	$T^{\circ}C = \frac{4410}{0.13.95 + \text{Log}\left(\frac{\text{K}^2}{\text{Mg}}\right)} - 273.15$